Modified Beta MPPT Method Based on Actual Climatic Data

Preprint · April 2019

DOI: 10.1145/3303714.3303746

Mohammad Sikander Ali
Hebei University of Technology

Arshad Nawaz
Shanghai Jiao Tong University

Modified Beta MPPT Method Based on Actual Climatic Data

Sikander Ali[1]
School of Electrical Engineering
Hebei University of Technology
No.8 Guangrong Road, Dingzigu,
Hongqiao District, Tianjin, China, 310300
+86-13132257131
201651401002@stu.hebut.edu.cn

Sheng Xue Tang[2]
School of Electrical Engineering
Hebei University of Technology
No.8 Guangrong Road, Dingzigu,
Hongqiao District, Tianjin, China, 310300
+86-18502640689
tsx@hebut.edu.cn

Jian Yu Zhang[3]
School of Electrical Engineering
Hebei University of Technology
No.8 Guangrong Road, Dingzigu,
Hongqiao District, Tianjin, China, 310300
+86-18843232869
1884323869@163.com

Arshad Nawaz[4]
Department of Automation
Shanghai Jiaotong University
194 HuaShan Road, Xuhui District,
Shanghai, China
+86-13262991271
arshadnawaz@sjtu.edu.cn

ABSTRACT
Maximum power point tracking (MPPT) technique is a method which is used in the photovoltaic power (PVS) to increase the power efficiency. The most important challenges facing conventional MPPT methods are oscillation during steady state and slow power tracking during dynamic state because of getting fixed step size during tracking. The Beta method can handle these challenges using intermediate parameter "Beta" to get variable step size in transient state. However, for higher efficiency, some of the parameters of this method need to be optimized. The main objective of this research is to minimize oscillation in steady state and to tracks rapidly the maximum power in the transient state. Necessary climatic information such as highest, average irradiance and temperature levels are taken from 1-year climatic data set of Karachi city to set up Beta limits. A PLECS model of the modified beta method with the boost converter is proposed and simulated which shows excellent results

CCS Concepts
• CCS→ Hardware→ Power and energy→ Energy generation and storage→ Renewable energy.

Keywords
Step size; Scaling Factor; PLECS; Boost Converter; Beta Method.

1. INTRODUCTION
The Recently, the use of renewable energies such as Photovoltaic, Wind, tidal etc. has increased dramatically for a lot of advantages such as low down dependency on biomass, decrease in CO2 emission, fuel prices and unusual shutdown of centralized grids. Solar energy based photovoltaic system is one of the promising natural, free, clean, reliable and renewable energy source. However, an important challenge in the photovoltaic system is to extract maximum power under different irradiance and temperature levels to improve the output power efficiency of PV arrays.

RCAE 2018, December 26–28, 2018, Beijing, China

ACM ISBN 978-1-4503-6102-6/18/12…$15.00
https://doi.org/10.1145/3303714.3303746

A photovoltaic power system mainly consists of three major parts: Photovoltaic arrays, a Power electronics converter and the load or Grid. Figure 1 shows the block diagram of a typical PV system using a DC-DC converter, where G and T are irradiance and temperature, Vpv, Ipv and V_{LOAD}, I_{LOAD} are PV and converter output voltages and currents, respectfully. MPPT is used to regulate the duty ratio 'd' of the converter, harvest maximum power from the PV panel and deliver the power to the load R_{Load}.

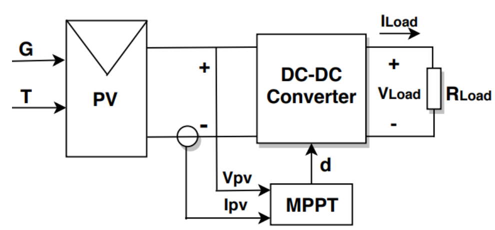

Figure 1. General scheme for MPPT controlled photovoltaic power system.

During the last decade, numbers of different MPPT methods such as Hill-Climbing (HC) method [1], Perturb and Observe (P&O) [2-4], Incremental Conductance (Inc. Cond.) method [5-6], Temperature method [7], Fixed duty cycle and Constant voltage (VCTE) [8] or Open voltage method [11] and feedback voltage (current) methods [12] are proposed, documented and implemented. Among them, the fixed duty cycle is the simplest of above methods and just need to adjust the load once at the start and it also does not require any feedback controller. The constant voltage method is another simple method used in such regions where the variation in temperature is less. The main idea used in this method is the variation in terminal voltage at different MPP which is very little even the solar intensity varies, but it varies as the temperature changes. An interesting point in the fixed voltage method is that it only requires a voltage sensor to find out MPP. However, fixed duty cycle is less efficient in terms of extracted power and VCTE method generates appreciable oscillations in steady-state [9]. The Temperature control method utilizes a temperature sensor to record the change in temperature while upholding the MPP. However practically, this method could have issues such as: irregular distribution of solar energy on each cell, incorrect measurements, and badly calibration. Furthermore, if any of PV parameters are changed due to the system aging, the algorithm has to be updated to ensure the correct operation. [10].

Voltage (current) feedback method requires only one feedback control which reduces cost and complexity. However, this method does not consider variation in temperature and solar insolation [13]. Authors in [31] found interest in current and temperature based MPPT control which increases efficiency up to 99.85%, nevertheless, whenever there is considerable change in climatic conditions it requires disconnection of load to measure short circuit current (ISC). Another paper [32] evaluated the temperature control of PV panels and, from the energy point of view, the system presented good results. Conversely, this method has the dependency on pumps [32]. Among all the MPPT methods, HC, P&O and Inc. Cond. methods are still widely used because of less system complexity, required less information to track peak power [14]. The P&O technique based on the following criteria: the algorithm perturbs both the voltage and current of PV panel at different operating points, and periodically regulate the panel output power by increasing or decreasing the output panel voltage by perturbation step size while HC method shares the same idea as P&O, but it perturbs the duty cycle of DC-DC converter [15]. The number of perturbation made by MPPT algorithm per second is called perturbation frequency or MPPT frequency [3]. The drawback of P&O and HC method is that after reaching at Maximum power point (MPP), the algorithm stuck in a trick and continues to perturb around MPP which results in more power loss. Reducing the perturbation step size reduce system oscillation during steady state and also minimize power loss while affecting the settling time to reach MPP. According to [16], the periodic difference of power with respect to the change in voltage is calculated in P&O and HC method while Incremental Conductance method lies on the fact that the sum of instantaneous conductance (I/V) and the incremental conductance ($\Delta I/\Delta V$) is zero at the MPP, negative on the right and positive on the left of Power Vs Voltage curve. The authors in [6] also concluded that maximum power tracking efficiency increased by 11.5 % of the P&O method using Incremental conductance technique.

The problems associated with Incremental Conductance discussed in earlier research is the fixed iteration step size which results in poor steady tracking accuracy and also affects dynamic response, a new modified method using the PI controller and variable step size is proposed[17]. Researchers in [18] proposed an algorithm for the grid-connected solar power system using a combined variable step Inc. Conductance and constant voltage method. Tong Yao and Raja Ayyanar in [19] proposed an excellent method named Maximum voltage unit guided MPPT algorithm to find global maximum power point (GMPP) during partial shading conditions. However, this method is suitable for substrings in PV systems and well suited for micro inverters application. All the modified MPPT methods use the idea of large step size for rapid tracking in the transient state and small step size to control oscillation during steady state. A variable step size P&O MPPT is documented in [20] and compared with the fixed step size P&O method with and without the PI controller. The variable step size is mentioned in [20] as:

$$V\_step = dV \times |\Delta P| \tag{1}$$

where dV is the fixed step size and ΔP is the change in generated power. Automatic adjustment of the step size using change in power w.r.t. change in duty cycle ratio along with scaling factor presented in [21] as:

$$dV = N \times (P - Pprev)/(D - Dprev) \tag{2}$$

Here, dV represents variable step size, N is the scaling factor, $P, D,$ and $Pprev, Dprev$ represents current and previous instant power and duty cycle, respectively. Though, this method shows good results only under narrow operating environmental conditions. A digital MPPT controller based on the adaptive perturbation frequency proposed in [22] which increase tracking accuracy. Furthermore, Many other hybrid techniques using intelligent methods such as: Fuzzy logic (FL), Particle Swam optimization (PSO), Genetic Algorithm (GA) and, Artificial Neural network (ANN) combined with conventional MPPT documented in the literature and shows good results, however, these techniques needed much knowledge and information to train digital controller [23-30].

S. Jain and V. Agarwal proposed a rapid method to track MPP [33] which based on the fact that MPP has no direct relation with the duty ratio and, instead of tracking power an intermediate variable "Beta (β)" can be calculated which has a monotonically increasing one-to-one relationship. Furthermore, this method is designed and implemented by researchers and shows goods results in the fast-changing environment [34-36]. Authors in [37] proposed an improved beta method and considered beta as temperature independent, though it must be pointed out that beta depends on PV cells temperature as well. Nevertheless, for optimal performance, some of its parameters such as scaling factor and beta limits need to be optimized for environmental conditions.

This paper addresses a new way to calculate the scaling factor and variable step size for the beta method. Thus a modified beta method is proposed and simulated on the basis of actual climatic data of Karachi city, Pakistan in PLECS software. The 2nd section discusses the modeling for the PV panel. Section III provides the detail of the modified algorithm. Section IV and V analyzes the simulation results and conclusion, respectively.

2. MODELING OF THE SINGLE DIODE PV MODULE

Figure 2 shows the practical model of the single diode PV cell modeled in PLECS where *G* and *T* represent Irradiance and Temperature, respectively.

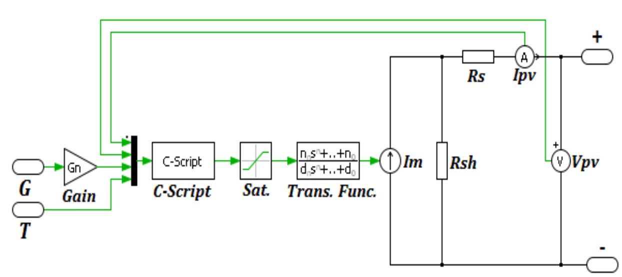

Figure 2. PLECS model of single diode PV cell

C-Script is used to execute custom C-code which takes *G*, *T*, I_{pv}, and V_{pv} as the input variables and controls the current source (*Im*). *Sat.* and *Trans. Func.* blocks represent Saturation and Transfer function, respectively. The upper and lower limits of *Sat.* block set as Infinity (inf.) and zero, respectively, while *Trans. Func.* is $\frac{1}{t_{delay}+1}$ and t_{delay}configured as $1e^{-5}$ seconds. The corresponding non-liner output PV current-voltage (I_{pv}-V_{pv}) equation is given as below [38]:

$$I_{pv} = I_{ph} - I_o\left[e^{\left(\frac{V_{pv}+R_s I_{pv}}{V_t\alpha}\right)} - 1\right] - \frac{V_{pv}+R_s I_{pv}}{R_{sh}} \qquad (3)$$

where I_{ph} is the photovoltaic current of a single cell, I_o is the reverse saturation current of the diode, α is the diode ideality factor, $V_t = \frac{KT}{q}$ is the thermally generated voltage of a single PV cell, R_s and, $R_{sh}$are the series and shunt resistance respectively. In case of a PV module, $V_t = \frac{\text{NsKT}}{q}$ where Ns is the number of PV cells in series, K = 1.38 x 10 e^-23 J/K is the Boltzmann's constant, T is the p-n junction temperature in Kelvin, and q = 1.602 x 10 ^ -19 C is the charge on electron.

In this research, the Kyocera KC200GT module's specification is used as the PV generator shown in Table I and modeled according to the algorithm proposed in [38] in PLECS. Fig. 3a and 3b shows the effect of temperature and irradiance on the output voltage and current of the Kyocera 200GT PV module, respectively. However, series resistance(R_s)and shunt resistance(R_{sh}) values are needed to model the PV module and were found in [39] as 0.221Ω and 415.405, respectively.

Table 1. Specifications of Kyocera module KC200GT at STC (G=1000 W/m^2, T=25 ℃, and A.M = 1.5)

Maximum Power (Pmp)	200 W
Max. power voltage (Vmp)	26.3 V
Max. power current (Imp)	7.61 A
Open circuit voltage (Voc)	32.9 V
Short circuit current (Isc)	8.21 A
Temperature coefficient of Voc (Kv)	-0.1230 V/K
Temperature coefficient of Isc (Ki)	0.0032 A/K
No. of series cells (Ns)	54

3. PROPOSED BETA METHOD

3.1 Theory of Beta Method

Beta method is an approximation to calculate actual MPP within few iteration and works in two stages. In the first stage (Stage 1), the algorithm checks beta limits ($\beta min < \beta < \beta max$) and rapidly brings operating points (OPs) close to MPP range by offering variable step size. The rapid tracking does not compromise the accuracy and switches to the second stage (Stage 2) where the algorithm utilizes any conventional MPPT method (HC, P&O, Inc. Cond.) which tracks actual power smoothly using minimum fixed step size. Once the OPs are within MPP range, conventional MPP does not require long time to track actual MPP which increases overall efficiency of the system. The equation for calculating the beta parameter illustrated by S. Jain and V. Agarwal in [33] as:

$$\beta = \ln\left(\frac{I_{pv}}{V_{pv}}\right) - CV_{pv} \qquad (4)$$

where β is the intermediate variable. V_{pv}, I_{pv} are the output PV module's voltage and current respectively, and $C = 1/V_t$ is the inverse of Module's thermal voltage.

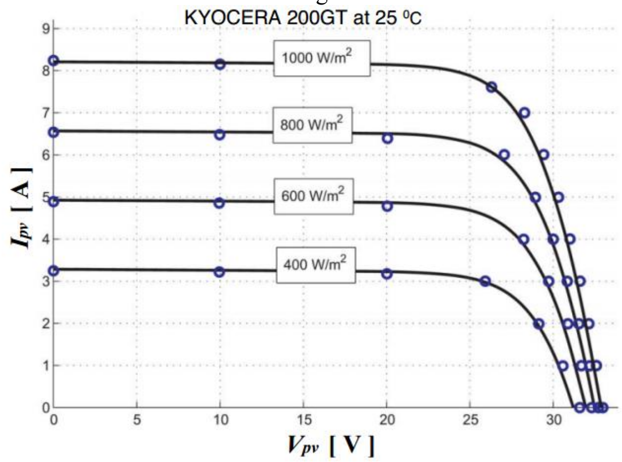

(a)

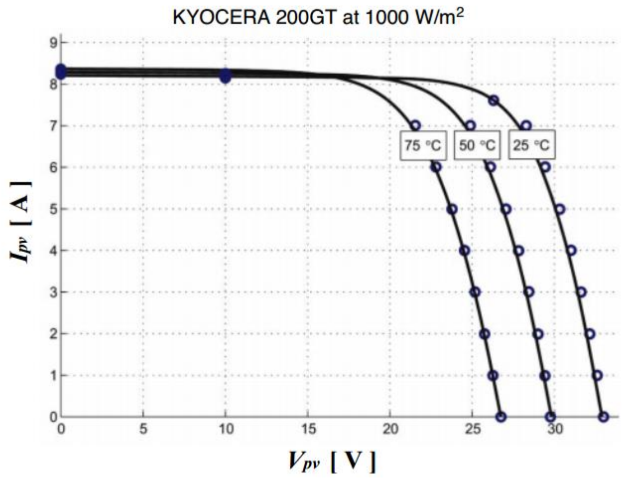

(b)

Figure 3. I_{pv}-V_{pv} Model curves of KYOCERA KC200GT Module at (a) 25℃ and different irradiance (b) 1000 W/m^2 and different temperature

3.2 Proposed Method

Fig. 4. shows the flowchart of the proposed beta MPPT algorithm. The algorithm initiates by sensing the present values of V_{pv}, I_{pv} and, temperature (*T*) from PV panel. Similar to the original Beta method, firstly the algorithm compares whether β is within the range of minimum (βmin) to maximum values (βmax) which is calculated as shown in Table II. If the algorithm satisfies the range of β, algorithm switches to stage 2 and utilizes HC method to increase efficiency during steady state by setting the scaling factor (N) and variable step size (ΔD) to zero itself. If the condition ($\beta min < \beta < \beta max$) is untrue, which means MPP is far from the current point, the MPPT algorithm switches to the first stage. In the first stage, the algorithm compares the present β withβmin, and tunes the scaling factor N automatically. The auto-tuning of scaling factor is done using the division of factor $\Delta Dmin$ or $\Delta Dmax$ by summation of previous (β_{prev}) and average value (β_g) of β. This auto-generated scaling factor generates variable step size ΔD. ΔD will be added to previous stored value of duty ratio $dprev$ by the algorithm to adjust the duty cycle (d). The division of $\Delta Dmin$ is used when the condition $\beta < \beta min$ satisfies,

otherwise $\Delta Dmax$ is exploited. In the proposed method, $dprev$ represents previous value of duty ratio and $\beta_g = \beta min + \beta max/2$. Afterward, the values of $\Delta Dmin$ and $\Delta Dmax$ need to be

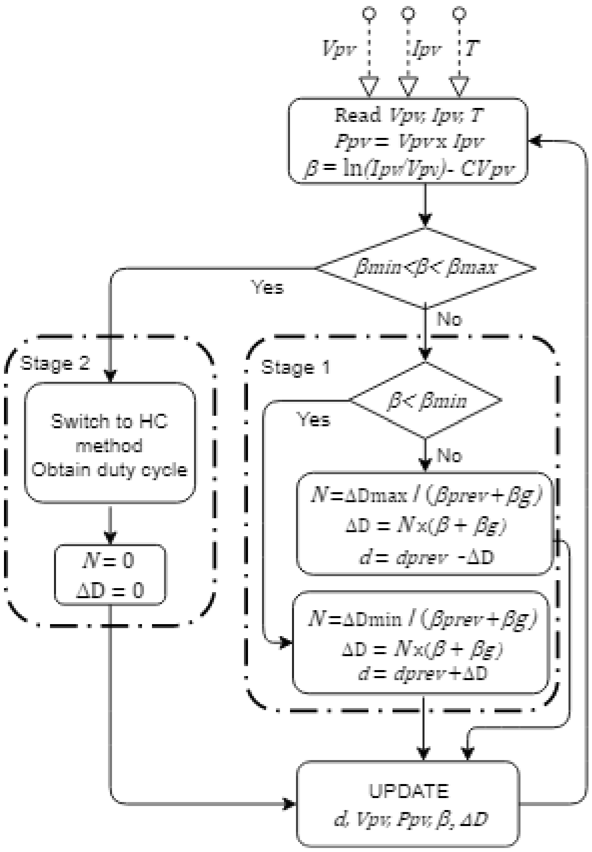

Figure 4. The flow chart of proposed beta method

optimized for auto-tuning the scaling factor. To minimize the oscillation during steady state, a small fixed step size (Δd) of 0.001 is used in this research. However, Δd depends on V_{pv} variations as well as designer's analysis of MPPT system. The utilization of HC method is preferred because it perturbs duty cycle which means this method directly provides duty ratio rather than using PI controller or external voltage controller to obtain duty ratio as in P&O and Inc. Cond. methods. The selection of $\Delta Dmin$ and $\Delta Dmax$ will be discussed in the later section.

4. SIMULATION RESULTS AND DISCUSSION

4.1 Calculation of Limits of β (βmin and βmax)

In the implementation of the Beta method, the range of βmin and βmax needs to be identified and, the algorithm calculates β_g itself. 1-year climatic data of Karachi city is used in this research which is available on energydata.info webpage to calculate different values of β as well as limits of β($\beta min$and βmax). Some peak and average values of corresponding data are used and the peak irradiation noted on 28-Aug-2016 which was 1108 Watt/m^2 shown in (S. No. 1) Table II. However, it is also noted from (S. No. 2) Table II that the value of β is found maximum at G = 1057 Watt/m^2 and T = 33.1°C which clearly shows β not only depends on temperature as well as on irradiance. Hence, the value of βmin and βmax calculated as -16.31 and -14.98, respectively.

Table 2. Calculated values of Beta (β) and the output power (P_{pv}) w.r.t. irradiance and temperature of Karachi city

S. No.	G ($Watt/m^2$)	T (°C)	V_{pv} (V)	I_{pv} (A)	P_{pv} (Watt)	β
1	1108.5	35.6	24.80	8.47	210.2	-15.02
2	1057	33.1	25.55	7.53	203.7	-14.98
3	977.7	31.3	25.53	7.42	189.6	-15.13
4	821	29.2	25.72	6.23	160.3	-15.52
5	646.4	26.6	25.95	4.88	126.8	-15.96
6	504.5	27.8	25.56	3.80	97.2	-15.98
7	463	26.6	25.21	3.54	89.2	-16.28
8	295.6	24.4	24.7	2.25	55.6	-16.31

4.2 The Practical Boost Converter and Complete Simulation Model

Fig. 5 shows the practical model of the Boost converter which the output PV voltage Vout is up to 48V. Fig. 6 shows the entire simulation model of the proposed beta MPPT method with the PV module and the Boost converter. The values of converter parameters are calculated according to R. Ayop and C. W. Tan in [40] as shown:

- Input Capacitor Cin = 40 µF
- Input and output capacitor ESR & ESR0= 0.001Ω
- Inductor L = 1.7135 mH
- Inductor's resistance RL = 0.001 Ω
- Output Capacitor C0 = 400 µF
- Semiconductor switch = IGBT
- Switching frequency fs = 10Khz
- Load Resistance R = 11.55 Ω
- Total time of simulation t = 17s
- D = Diode with no losses
- Vpv = Input voltage or Output PV voltage

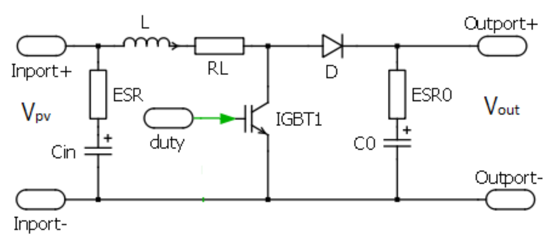

Figure 5. The practical model of boost converter

4.3 Selection of delDmin ($\Delta Dmin$) and delDmax ($\Delta Dmax$)

From the algorithm presented in fig. 4, $\Delta Dmin$ and $\Delta Dmax$, respectively, are the corresponding factors to tune the scaling factor automatically whenever β goes far of βmin or βmax limit. Improper selection of parameters $\Delta Dmin$ and $\Delta Dmax$ cause variations or slow down tracking speed during the transient state which results in fluctuation and losses in output power.

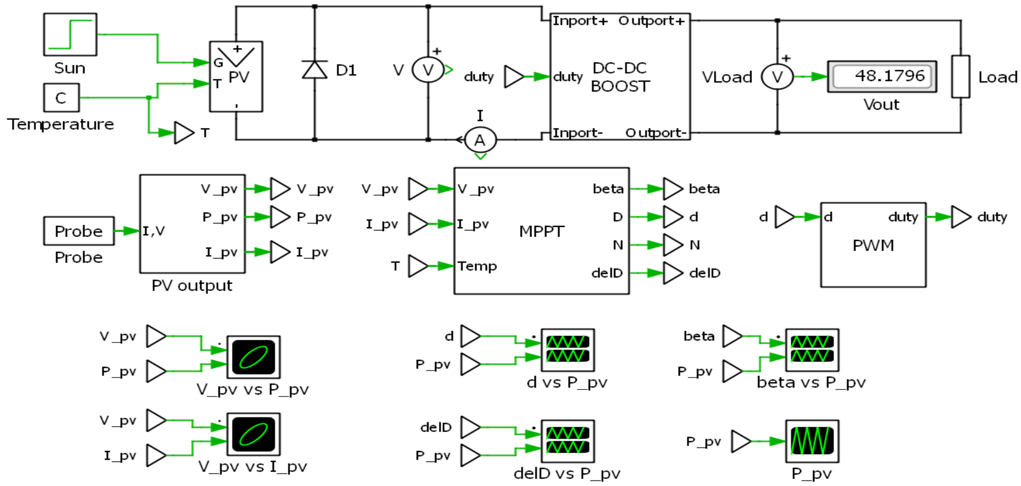

Figure 6. Complete model of the PV system

To select the optimal values of $\Delta Dmin$ and $\Delta Dmax$, different values were tested. Fig. 7 shows the transient time response (algorithm switch to stage 1) for $P_{pv}$and variable step size delD (ΔD). Transient response time for P_{pv}in fig. 7(a) found about0.21s when $\Delta Dmin$ and $\Delta Dmax$ values of 0.1 and 0.5 were used, respectfully. Noticeable variations presents in P_{pv} with these values. Fewer variations presents in P_{pv} when $\Delta Dmax$ =0.05 $\Delta Dmin$=0.001were used as shown in fig. 7(b), while the time to reach steady-state is increased. $\Delta Dmax$ and $\Delta Dmin$ should be between 50 to 80 times and 5 to 10 times of Δd, respectively. Therefore, the optimal values of $\Delta Dmax$ and $\Delta Dmin$ used in this research are 0.07 and 0.005, respectively, shown in fig. 7(c).

4.4 The Practical Boost Converter and Complete Simulation Model

Initially the irradiance is 1000$Watts/m^2$, at time t=3s it changed to 700 $Watts/m^2$. At time t = 6s, irradiance increased to 1200$Watts/m^2$ and again decreased to 1100$Watts/m^2$at t=9s. Change in the irradiance cause a change in output power and the guiding beta is presented in fig. 8a and 8b, respectfully. During these dynamic states, the value of variable step size Δ D continuously changes until the algorithm switch to stage 2 depicted in figure 8c.

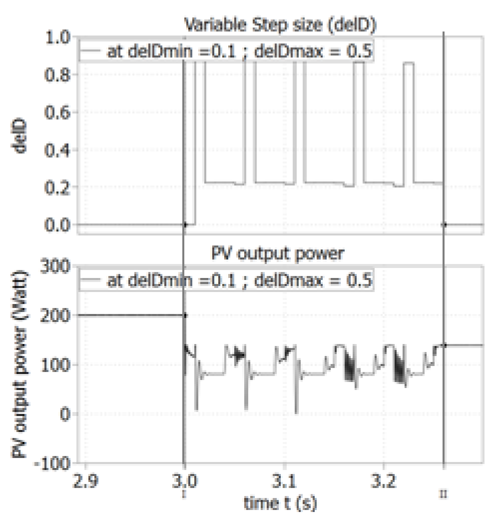

(a)

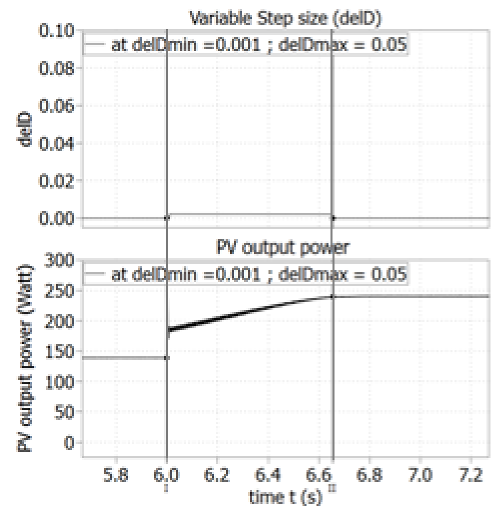

(b)

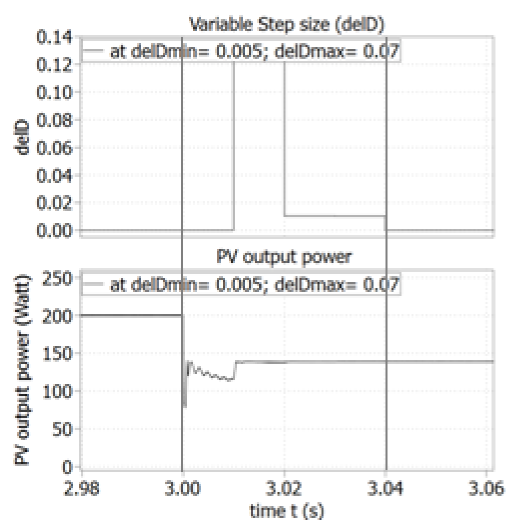

(c)

Figure 7. Transient response time for $P_{pv}$and ΔD when (a). $\Delta Dmax$ = 0.5 & $\Delta Dmin$ = 0.1 (b). $\Delta Dmax$ = 0.05 & $\Delta Dmin$ = 0.001 (c). $\Delta Dmax$=0.07 & $\Delta Dmin$=0.005

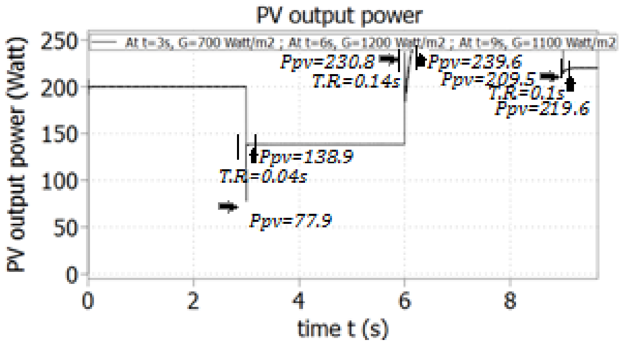

(a)

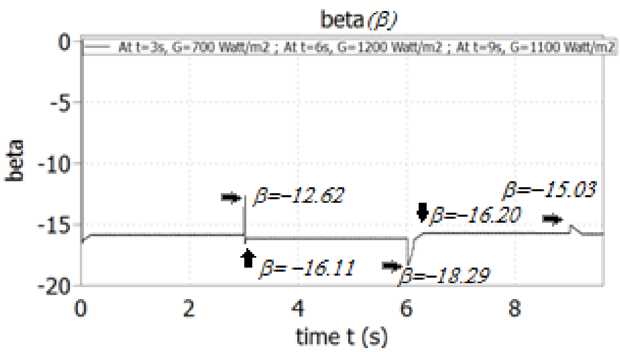

(b)

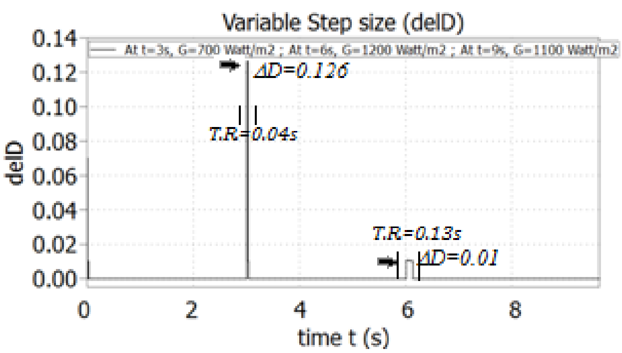

(c)

Figure 8. Effect of irradiance change on (a) output PV power P_{pv} (b) beta β (c) variable step size ΔD

When sudden change in irradiance occurs at t= 3s, P_{pv}goes down to 77.9 Watt (fig. 8a), which causes change in β to -12.62 that is higher than βmax (fig. 8b). A variable step size value of ΔD= 0.126 is applied by algorithm (fig. 8c) during this transient time for T.R. = 0.04s which brings P_{pv} to its maximum power P_{pv} =138.9Watt. Then, β becomes -16.11 that satisfies the condition ($\beta min < \beta < \beta max$) while ΔD become zero after the transient time (fig. 8c).

Similarly at t=6s in fig. 8a, irradiance increases to 1200$Watts/m^2$ and P_{pv}generated is 230.8Watt, which changes the value of β to -18.29 in fig. 8b that is lower than βmin limit. ΔD of value 0.01 is applied in fig. 8c for T. R. = 0.13s which increases P_{pv}= 239.6 Watt and brings β= -16.20 within its limits (βmin<β<βmax), hence output power efficiency is increased. After the dynamic time of 0.13s, ΔD again becomes zero which means algorithm switches to Stage 2.

At t=9s in fig. 8a, irradiance again decreases to 1100$Watts/m^2$ and generates P_{pv} of 209.5Watt. In fig. 8b, it can be noticed that β changes to -15.03 that is within βmin < β< βmax . The algorithm remains in Stage 2, hence, there is no change in value of ΔD = 0 (fig. 8c) and takes T. R. =0.1s to achieve the maximum power of 219.6 Watt (fig. 8a). It is worth mentioning here that T. R. for $P_{pv}$and ΔD can be different as shown in fig. 8a and 8b, respectively, when irradiance change to 1200 $Watts/m^2$ at t=6s . The reason of different T.R. is that ΔD only changes when β locates outside βmin < β< βmax limits.

At t=9s in fig. 8(a), irradiance again decreases to 1100$Watts/m^2$ and generates P_{pv} of 209.5Watt. In fig. 8(b), it can be noticed that β changes to -15.03 that is within βmin < β < βmax . The algorithm remains in Stage 2, hence, there is no change in value of ΔD = 0 (fig. 8(c)) and takes T. R. =0.1s to achieve the maximum power of 219.6 Watt (fig. 8(a)). It is worth mentioning here that T. R. for $P_{pv}$and ΔD can be different as shown in fig. 8(a) and 8(b), respectively, when irradiance change to 1200 $Watts/m^2$ at t=6s . The reason of different T.R. is that ΔD only changes when β locates outside βmin < β< βmax limits.

Fig. 9 shows the duty cycle (d) regulation for whole simulation. Fig. 10 provides results of irradiance change in values of P_{pv},β, ΔD from t= 9s to t=17s.

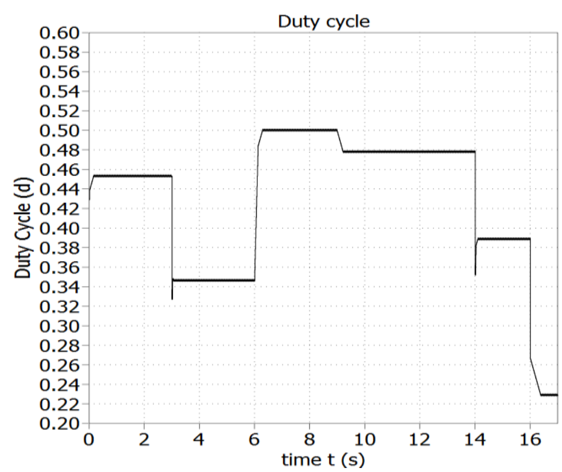

Figure 9. The duty cycle (d) regulation for whole simulation

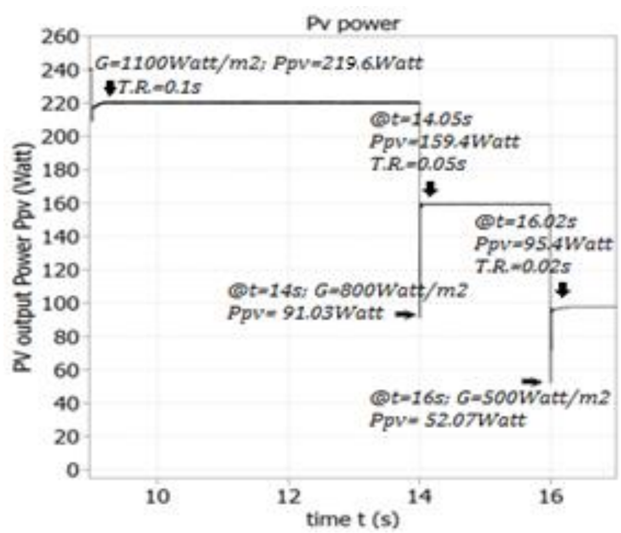

(a)

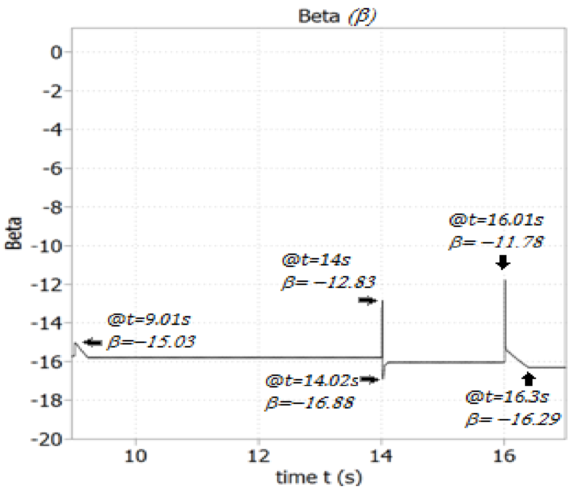

(b)

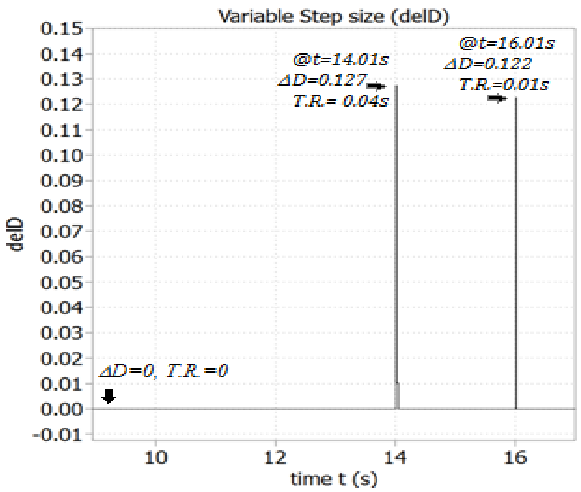

(c)

Figure 10. Results of irraidance (G) change in values of β, P_{pv} and ΔD from simulation time t= 9s to t=17s

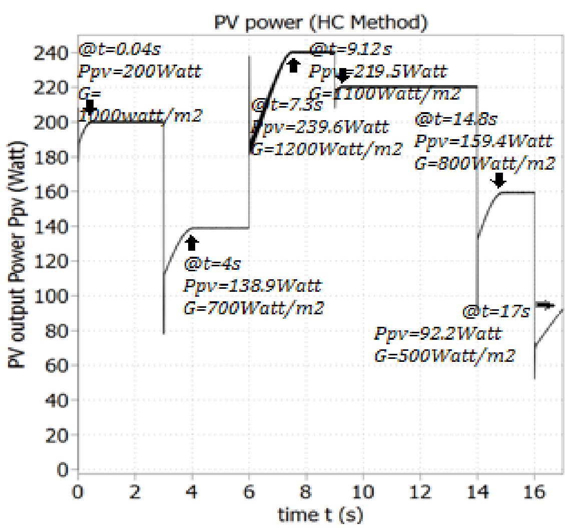

(a)

4.5 Comparative Result

Figure 11 and Table III shows comparative results for P_{pv}(to reach MPP at time t) between the HC, Beta and, proposed methods providing fixed step size of d=0.001. It is observed that the HC method's (figure 11a) transient time is greatest among all. Beta method (figure 11b) shows quick response to reach MPP as compared to HC method. P_{pv} obtained from the proposed method (figure 11c) is less fluctuated and the method is quickest to respond comparing above two methods during any sudden irradiance changes.

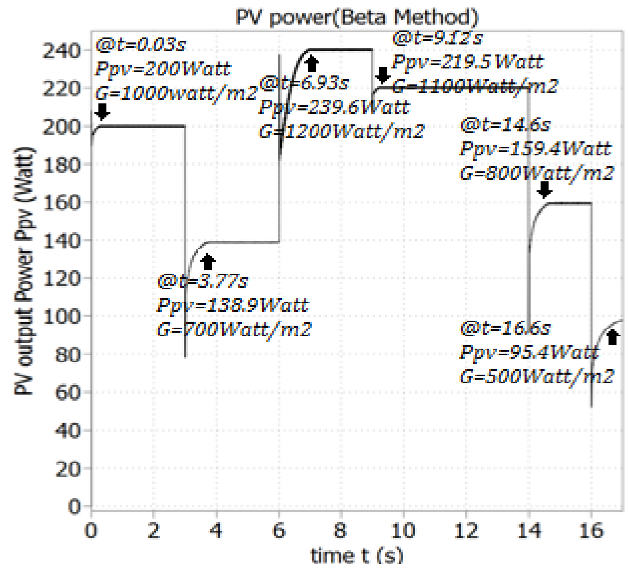

(b)

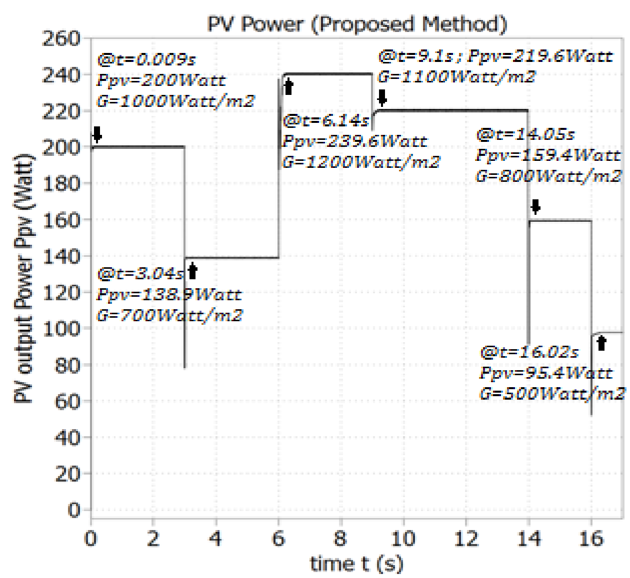

(c)

Figure 11. Simulation results comparison for P_{pv}between (a) The HC method (b) Beta method (c) Proposed MPPT Method

Table 3. Comparative results between HC, Beta, and the proposed method for P_{pv} during irradiance change at different simulation time

Time t at G change (s)	G change to $(Watts/m^2)$	P_{pv}at MPP $(Watt)$	HC Method		Beta method		Proposed method	
			Time t at MPP (s)	$T.R.$ = Time t at MPP- Time t at G change (s)	Time t at MPP (s)	$T.R.$ = Time t at MPP- Time t at G change (s)	Time t at MPP (s)	$T.R.$ = Time t at MPP- Time t at G change (s)
0	1000	200	0.04	0.04	0.03	0.03	0.009	0.009
3	700	138.9	4	1	3.77	0.77	3.04	0.04
6	1200	239.6	7.3	1.3	6.93	0.93	6.14	0.14
9	1100	219.5	9.12	0.12	9.12	0.12	9.10	0.10
14	800	159.4	14.8	0.8	14.6	0.6	14.05	0.05
16	500	95.4	Not achieve MPP till t = 17s		16.6	0.6	16.02	0.02

5. CONCLUSION

In this paper, a simple modified intermediate parameter based Beta MPPT method is proposed and implemented using the DC-DC boost converter in PLECS software. A general guideline for implementing the proposed method and the results obtained from simulation is presented. It is necessary to calculate limits of Beta and care must be taken while setting up the factors namely $\Delta Dmin$ and $\Delta Dmax$ for generating auto-scaling factor. Furthermore, the proposed method is compared with the HC and Beta methods and shows rapid response and less oscillation in output PV power during sudden irradiance changes. The proper parameters selection can lead up to maximum power efficiency of 99% using proposed method.

6. REFERENCES

[1] M. I. Bahari, P. Tarassoudi, Y. M. Naeni, A. K. Khalilabad, and P. Shirazi. 2016. *Modeling and Simulation of Hill Climbing MPPT Algorithm for PhotoVoltaic Application*, Int. Symposium on Power Electron., Electr. Drives, Automation and Motion, pp 1041-1044, (2016)

[2] L. Qin and X. Lu 2012. *Matlab/Simulink-Based Research on Maximum Power Point Tracking of Photovoltaic Generation*, 2012 Int. Conference on Appl. Phys. and Ind. Engg., Phys. Procedia 24, 10 – 18 (2012).

[3] M. A. Elgendy, B. Zahawi, D. J. Atkinson 2012. *Assessment of Perturb and Observe MPPT Algorithm Implementation Techniques for PV Pumping Applications*, IEEE Trans. on sustainable energy, **Vol. 3**, No. 1 (2012) pp 21-33.

[4] N. Femia, G. Petrone, G. Spagnuolo, M. Vitelli. 2005. Optimization *of Perturb and Observe Maximum Power Point Tracking Method*, IEEE Trans. On power electron., **Vol. 20**, NO. 4 (2005), pp 963-973.

[5] A. R. Saxena, S.M. Gupta. 2014. *Performance Analysis of P&O and Incremental Conductance MPPT Algorithms under Rapidly Changing Weather Conditions*, J. Elect. Sys. **10-3** (2014): pp 292-304.

[6] S. Uma Ramani, S. Kumar, B. Arundhati. 2017. *Comparitive Study of P&O and Incremental Conductance method for PV System*, 2017 Int. Conf. on circuits Power and Comp. Tech. [ICCPCT] (2017).

[7] S. Elkelani Babaa, M. Armstrong, V. Pickert. 2014. *Overview of Maximum Power Point Tracking Control Methods for PV Systems,* Journ. of Power and Energy Engg (2014), **2**, pp 59-72.

[8] M. A.G. de Brito, L. G. Junior, L.P. Sampaio, G. A. e Melo, Carlos A. Canesin. 2011. *Main Maximum Power Point Tracking Strategies Intended for Photovoltaics*," IEEE, XI Brazilian power electron. Conf. (2011), pp 524-530.

[9] F. Lessa Tofoli, D. de Castro, W. Josais de Paula. 2015. *Comparative Study of Maximum Power Point Tracking Techniques for Photovoltaic Systems,* Int. Journal of Photoenergy Vol. **2015**, Article ID 812582, 10 pages (2015).

[10] R. F. Coelho, F. M. Concer, D. C. Martins. 2010. *A MPPT Approach Based on Temperature Measurements Applied in PV Systems*, 9th IEEE/IAS Int. Conf. on Ind. App., INDUSCON (2010).

[11] R. Faranda, S. Leva, P. Leonardo da Vinci. 2008. *Energy Comparison of MPPT Techniques for PV Systems*, WSEAS Trans. on Power Sys. (2008), **3**, 447-455.

[12] Salas, V., Olias, E., Barrado, A. and Lazaro. 2016. *Review of the Maximum Power Point Tracking Algorithms for Stand-Alone Photovoltaic Systems,*" Solar Energy Materials and Solar Cells, **90** (2016), pp 1555-1578.

[13] H. Islam, S. Mekhilef, N. Binti Mohamed Shah, T. Kok Soon, M. SeyedMahmousian , B, Horan, A. Stojsevski. 2018. *Performance Evaluation of Maximum Power Point Tracking Approaches and Photovoltaic Systems*, Energies 2018, **11**, 365, 2018.

[14] T. Esram and P. L. Chapman. 2007. *Comparison of Photovoltaic Array Maximum Power Point Tracking Techniques,*" IEEE Trans. on ENERGY conv., **VOL. 22**, NO. 2 (2007), pp 439-449.

[15] A. Haque. 2014. *Maximum Power Point Tracking (MPPT) Scheme for Solar Photovoltaic System*, Energy Tech. & Policy (2014), 1:1, pp 115-122.

[16] M. Aslam, A. Tariqa, S. Hameeda, M. Saad Bin Arifa, A. Jain. 2017. *Comparative assessment of maximum power point tracking procedures for photovoltaic systems,* Green Energy & Environment, vol. **2** (2017), pp 5-17.

[17] B. Liu, S. Duan, F. Liu, P. Xu. 2007. *Analysis and Improvement of Maximum Power Point Tracking Algorithm Based on Incremental Conductance Method for Photovoltaic Array*, IEEE 7th Int. Conf. on Power Electron. and Drive Sys. 2007, pp 637-641.

[18] L. Cuiping, Z. Junwu, L. Junhui, Y. Zhizhong.2016. *Grid-*connected *PV system modeling and control based on the variable step size of MPPT algorithm*, 2016 China Int. Conf. on Elect. Distribution (CICED 2016) Xi'an (2016), Paper No. CP1305.

[19] T. Yao, R. Ayyanar.2013. *Maximum-Voltage-Unit-Guided MPPT Algorithm for Improved Performance under Partial Shading*, 2013 IEEE Energy Conversion Congress and Exposition (2013), pp 2428-2434.

[20] K. Saidi, M. Maamoun, M. Bounekhla. 2017. *Simulation and analysis of variable step size P&O MPPT algorithm for photovoltaic power control*, 2017 Int. Conf. on Green Energy Conv. Sys. (GECS) (2017).

[21] F. Liu, S. Duan, F. Liu, B. Liu, and Y. Kang. 2008. *A variable step* size *Inc. MPPT method for PV systems*, IEEE Trans. Ind. Electron., vol. **55**, no. 7 (2008), pp. 2622–2628.

[22] Y. Jiang, J. A. Abu Qahouq, T. A. Haskew. 2013. *Adaptive step size with adaptive-perturbation-frequency digital MPPT controller for a single-sensor photovoltaic solar system*, IEEE Trans. on Power Electron., vol. **28**, no. 7 (2013), pp. 3195–3205.

[23] U. Yilmaza, A. Kircaya, S. Borekcib. 2018. *PV system fuzzy logic MPPT method and PI control as a charge controller*, Renewable and Sustainable Energy Reviews, Vol. **81**, Part 1 (2018), pp 994-1001.

[24] S. Narendiran, S. Kumar, R. Das, A. Kumar. 2016. *Fuzzy logic controller based maximum power point tracking for PV system*, IEEE 2016 3rd Int. Conf. on Elect. Energy Sys. (ICEES) (2016), pp 29-34.

[25] C. Robles Algarín, J. Taborda Giraldo, Omar Rodríguez Álvarez. 2017. *Fuzzy Logic Based MPPT Controller for a PV System*, Energies (2017), **10**, 2036, pp 2-18.

[26] Y. Liu, S. Huang, J. Huang, W. Liang. 2012. *A Particle Swarm Optimization-Based Maximum Power Point Tracking Algorithm for PV Systems Operating Under Partially Shaded Conditions*, IEEE Trans. on Energy conv., VOL. **27**, NO. (2012), pp 1027-1035.

[27] K. Ishaque, Z. Salam, M. Amjad, S. Mekhilef. 2012. *An Improved Particle Swarm Optimization (PSO)–Based MPPT for PV With Reduced Steady-State Oscillation*," IEEE Trans. on Power Elecrons., VOL. **27**, NO. 8 (2012), pp 3627-3638.

[28] S. Daraban, D. Petreus, C. Morel. 2014, *A novel MPPT (maximum power point tracking) algorithm based on a modified genetic algorithm specialized on tracking the global maximum power point in photovoltaic systems affected by partial shading*, ScienceDirect Energy, Vol. **74** (2014), pp 374-388.

[29] A.A. Kulaksız, R. Akkaya. 2012. *A genetic algorithm optimized ANN-based MPPT algorithm for a stand-alone PV system with induction motor drive*, Solar Energy, Vol. **86**, Issue 9 (2012), Pages 2366-2375.

[30] H. M. EL-HELW, A. MAGDY, M. I. MAREI. 2017. *A Hybrid Maximum Power Point Tracking Technique for Partially Shaded Photovoltaic Arrays*, IEEE Access, Vol. **5** (2017), pp 11900-11908.

[31] E. M. Vicente, R. L. Moreno, E. R. Ribeiro. 2015. *MPPT Technique Based on Current and Temperature Measurements*, Int. Journal of Photoenergy, Vol. **2015**, (2015), Article ID 242745,9 pages.

[32] N. M. M. da Rocha, D. C. Martins, J. César Passos. 2016. *MPPT Method Based on Temperature Control of the Photovoltaic Cells*, 2016 12th IEEE Int. Conf. on Industry Applications (INDUSCON), (2016).

[33] S. Jain and V. Agarwal. 2004. *A new algorithm for rapid tracking of approximate maximum power point in photovoltaic systems*, IEEE Power Electrons. Letter, vol. **2**, no. 1 (2004), pp. 16–19.

[34] M. A.G. de Brito, L. G. Junior, L.P. Sampaio, G. A. e Melo, C. A. Canesin. 2011. *Comparative Analysis of MPPT Techniques for PV Applications*, IEEE 2011 Int. Conf. on Clean Elect. Power (ICCEP) (2011), pp 99-104.

[35] K. P. J. Pradeep, C. C. Mouli, K. S. P. Reddy, and K. N. Raju. 2015. *Design and Implementation of Maximum Power Point Tracking in Photovoltaic Systems*, Vol. **4**, Issue 3 (2015), pp 37-43.

[36] M. A.G. de Brito, L. G. Junior, L.P. Sampaio, G. A. e Melo, C. A. Canesin. 2013. *Evaluation of the Main MPPT Techniques for Photovoltaic Applications*, IEEE Trans. on Industrial Electrons., Vol. **60**, NO. 3 (2013), pp 1156-1167.

[37] X. Li, H. Wen, C. H. Zhao. 2015. *Improved Beta parameter based MPPT method in Photovoltaic system*, 9th Int. Conf. on Power Electrons.-ECCE Asia (2015) , pp 1405-1412.

[38] M. G. Villalva, J. R. Gazoli, E. Ruppert F. 2009. *MODELING AND CIRCUIT-BASED SIMULATION OF PHOTOVOLTAIC ARRAYS*, Brazilian Journal of Power Electrons., vol. **14**, no. 1 (2009), pp. 35--45.

[39] M. G. Villalva, J. R. Gazoli, E. R. Filho. 2009. *Comprehensive Approach to Modeling and Simulation of Photovoltaic Arrays*, IEEE Trans. on Power Electrons., Vol. **24**, NO. 5 (2009), pp 1198-1208

[40] R. Ayop, C. Wei Tan. 2018. *Design of boost converter based on maximum power point resistance for photovoltaic applications*, Solar Energy 160 (2018), pp 322–335.